

Supporting Information

Ratiometric Emission Fluorescent pH Probe for Imaging of Living Cells in Extreme Acidity

Weifen Niu,^{†,‡} Li Fan,[†] Ming Nan,[†] Zengbo Li,[†] Dongtao Lu,[†] Man Shing Wong,^{†,§} Shaomin Shuang,[†] and Chuan Dong^{*,†}

[†] Institute of Environmental Science, College of Chemistry and Chemical Engineering, Shanxi University, Taiyuan 030006, People's Republic of China

[‡] Department of Chemistry and Chemical Engineering, Yangtze Normal University, Chongqing, Fuling 408100, People's Republic of China

[§] Department of Chemistry and Institute of Advanced Materials, Hong Kong Baptist University, Hong Kong SAR, People's Republic of China

Contents:

1. Calculation of Quantum Yield.
2. Cell Cytotoxicity Assay.
3. Supplementary Figures.

Figure S1. (a) Sigmoidal fitting of ratiometric fluorescence intensity ($F_{522\text{nm}}/F_{630\text{nm}}$) to various pH values (from 6.7 to 1.5). $\lambda_{\text{ex}} = 412$ nm. (b) Change of fluorescence spectra of QVBI at pH 6.7 and 1.5. $\lambda_{\text{ex}} = 488$ nm.

Figure S2. Change of fluorescence spectra of QVBI in the 10% cell medium with pH decreased from 6.7 to 1.5 ($\lambda_{\text{ex}} = 412$ nm). (Inset) Sigmoidal fitting of pH-dependent fluorescence intensity at 522 nm.

Figure S3. Changes in fluorescence intensity for QVBI with times at different pH.

Figure S4. Cell cytotoxic effect of QVBI on human renal carcinoma cells 7860.

Figure S5. The photostability measurement using confocal laser scanning microscope for BIU-87 cells.

Figure S6. The photostability curves under confocal laser scanning microscope for average fluorescence intensity in regions of interest 1-6 shown in Figure S5.

Figure S7. Comparison for the ratio of fluorescence intensity at green channel and red channel ($F_{\text{green}}/F_{\text{red}}$).

Figure S8. ^1H NMR spectra of QVBI.

Figure S9. ^{13}C NMR spectra of QVBI.

Figure S10. MALDI-TOF MS spectra.

4. References

1. Calculation of Quantum Yield

The quantum yield of QVBI was determined according to the following equation.¹

$$\Phi_x = \Phi_{st}(D_x/D_{st})(A_{st}/A_x)(\eta_x^2/\eta_{st}^2) \quad (1)$$

Where Φ_{st} is the quantum yield of the standard, D is the area under the emission spectra, A is the absorbance at the excitation wavelength and η is the refractive index of the solvent used. x subscript denotes unknown, and st means standard. We chose quinine sulfate solution ($\Phi = 0.577$ in 0.1 M H_2SO_4) as the standard.

2. Cell Cytotoxicity Assay

According to the literature,² the MTT (3-(4,5-dimethylthiazol-2-yl)-2,5-diphenyltetrazolium bromide) assay was used to test the cytotoxicity of QVBI to human renal carcinoma cells 7860. The cells with a density of 1×10^5 cells per mL were cultured in a 96-well microplate to a total volume of 100 μ L per well at 37 °C in a 5% CO_2 atmosphere. After 24h, different concentrations of QVBI of 0.01 μ M, 0.1 μ M, 1 μ M, 5 μ M, 10 μ M and 50 μ M were incubated with human renal carcinoma cells 7860 for 4 h in fresh medium, respectively. Cells in a culture medium without QVBI were used as the control. After washing the cells with cold phosphate buffered saline (PBS, pH 7.4) three times, 10 μ L of MTT solution (10 $mg \cdot mL^{-1}$, PBS) was added into each well of the 96-well microplate for another 4 h. Then, the remaining MTT solution was removed from the wells and 150 μ L of DMSO was added into each well to dissolve the intracellular blue-violet formazan crystals. The absorbance value of the solution was measured at 490 nm wavelength. The cell viability was calculated by the following equation:

$$\% \text{ viability} = [\sum(A_i/A_{\text{control}} \times 100)]/n \quad (2)$$

where A_i is the absorbance of different concentrations of the probe of 0.01 μ M, 0.1 μ M, 1 μ M, 5 μ M, 10 μ M and 50 μ M, respectively. A_{control} is the average absorbance of the control well in which the probe was absent, and n (=5) is the number of the data point.

3. Supplementary Figures

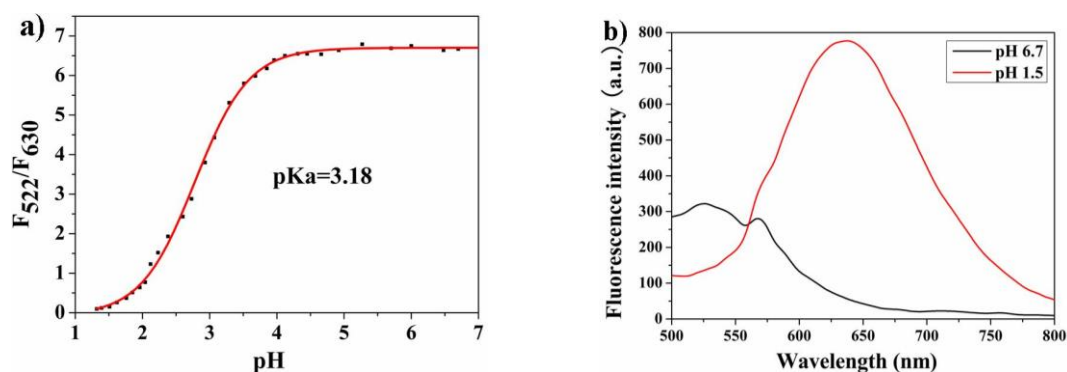


Figure S1. (a) Sigmoidal fitting of ratiometric fluorescence intensity (F_{522nm}/F_{630nm}) to various pH values (from 6.7 to 1.5). $\lambda_{ex} = 412$ nm. (b) Change of fluorescence spectra of QVBI at pH 6.7 and 1.5. $\lambda_{ex} = 488$ nm.

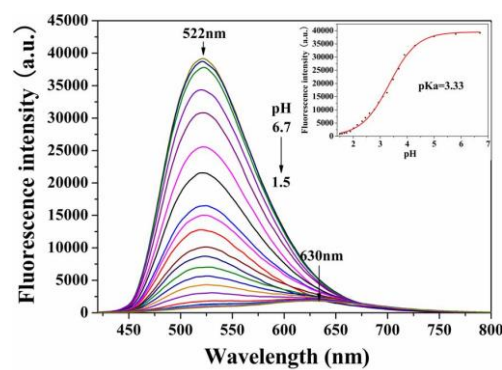


Figure S2. Change of fluorescence spectra of QVBI in the 10% cell medium with pH decreased from 6.7 to 1.5 ($\lambda_{\text{ex}} = 412 \text{ nm}$). (Inset) Sigmoidal fitting of pH-dependent fluorescence intensity at 522 nm.

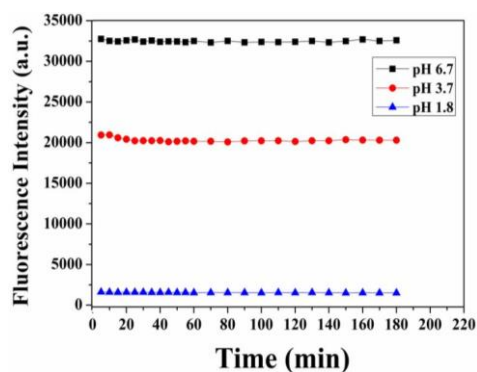


Figure S3. Changes in fluorescence intensity for QVBI with times at different pH ($\lambda_{\text{ex}} = 412 \text{ nm}$, $\lambda_{\text{em}} = 522 \text{ nm}$ at pH 6.7 and 3.7, $\lambda_{\text{em}} = 630 \text{ nm}$ at pH 1.8, respectively). Excitation and emission bandwidths were both set at 2 nm.

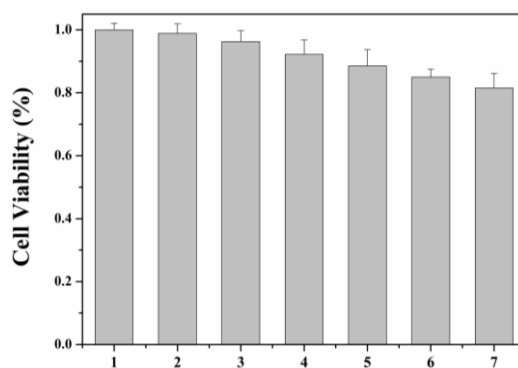


Figure S4. Cell cytotoxic effect of QVBI on human renal carcinoma cells 7860. 1, control; 2, 0.01 μM ; 3, 0.1 μM ; 4, 1 μM ; 5, 5 μM ; 6, 10 μM ; 7, 50 μM . Data are expressed as mean values standard error of the mean of five independent experiments.

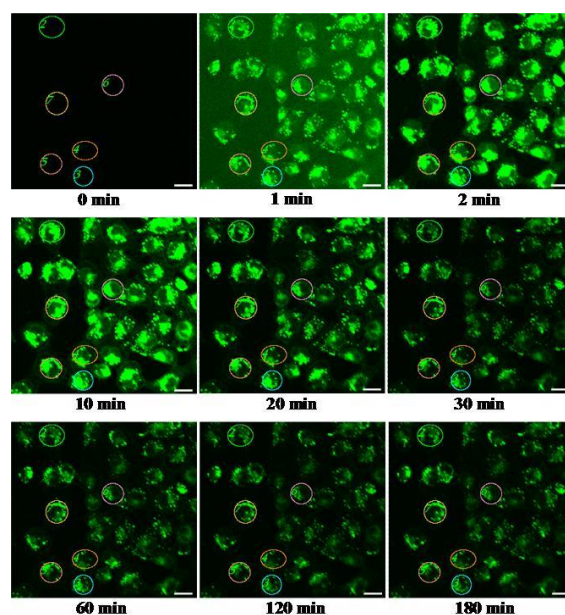


Figure S5. The photostability measurement using confocal laser scanning microscope for BIU-87 cells. Excitation wavelength was 405 nm, and emission was collected in the green channel (500-550 nm). Scale bar: 20 μm .

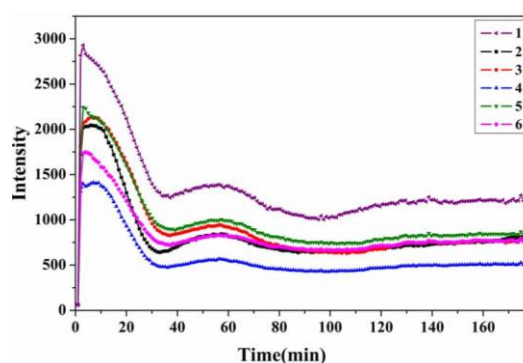


Figure S6. The photostability curves under confocal laser scanning microscope for average fluorescence intensity in regions of interest 1-6 shown in Figure S5.

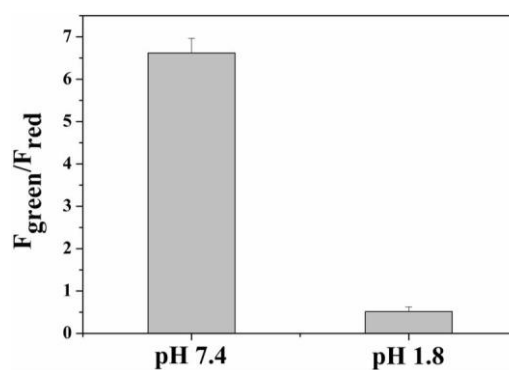


Figure S7. Comparison for the ratio of fluorescence intensity at green channel and red channel ($F_{\text{green}}/F_{\text{red}}$). Data are expressed as mean standard deviation (selected 7 *E. coli* cells).

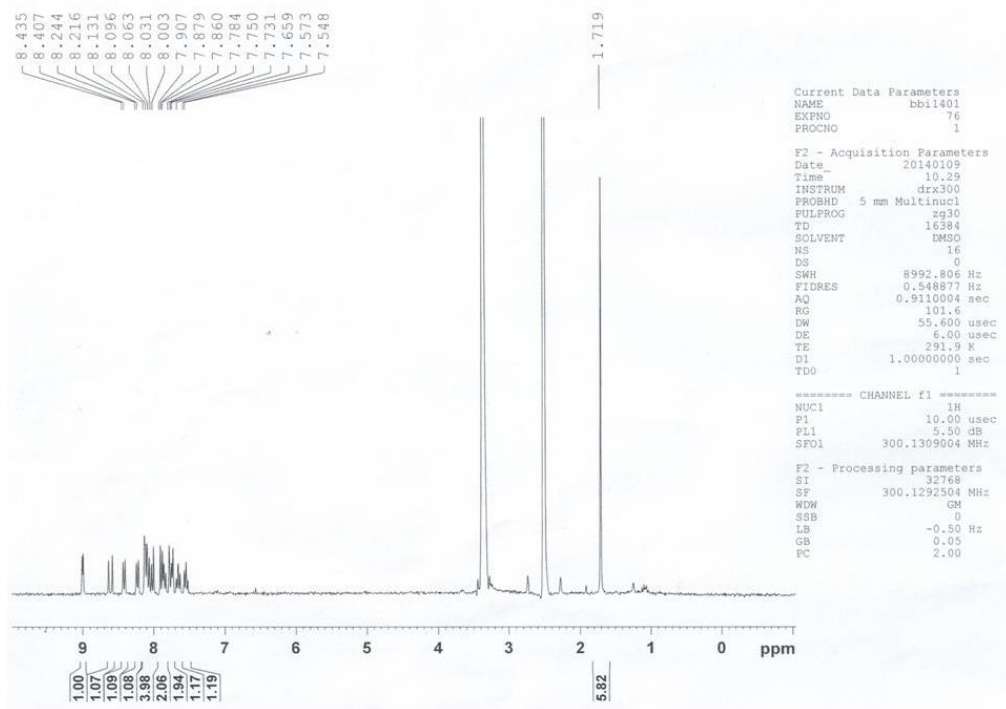


Figure S8. ^1H NMR spectra of QVBI.

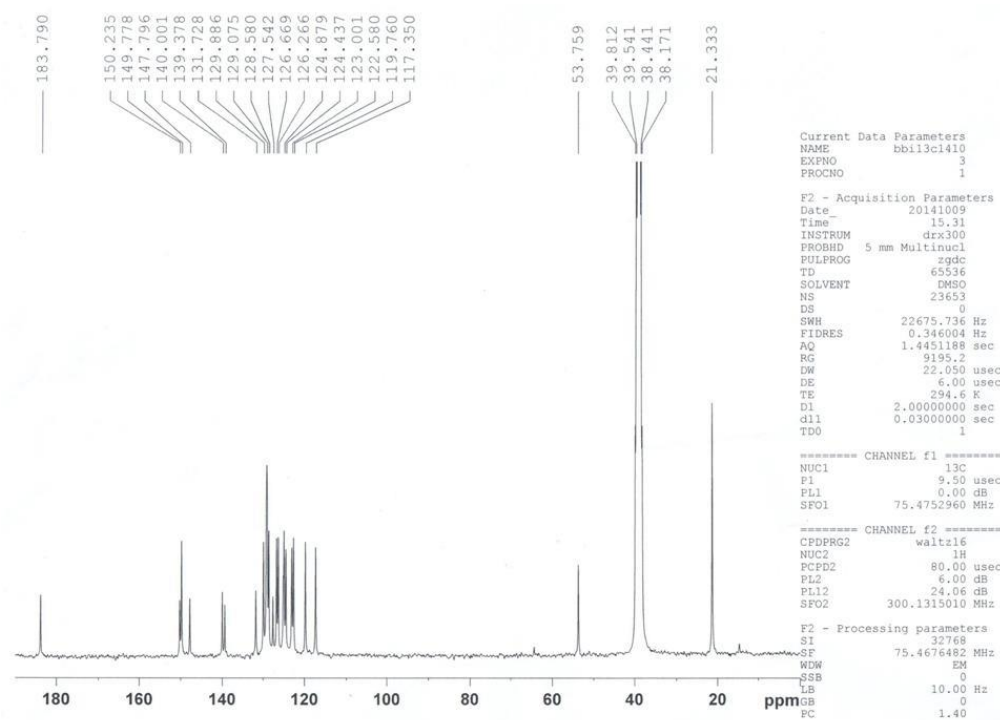


Figure S9. ^{13}C NMR spectra of QVBI.

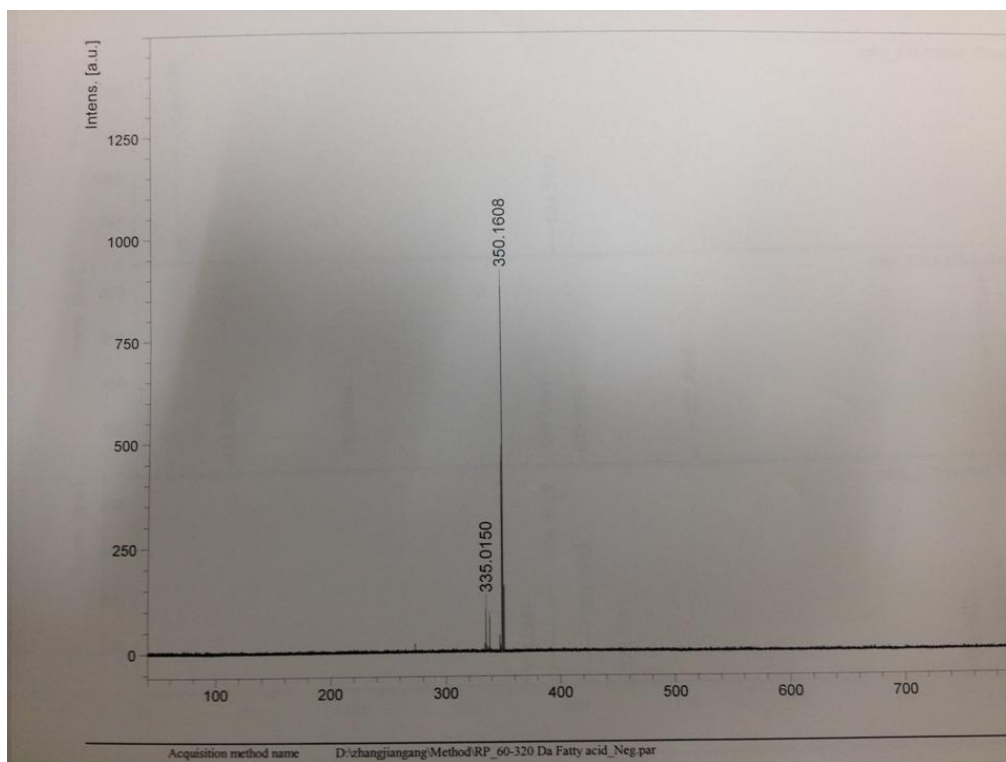


Figure S10. MALDI-TOF MS spectra.

4. References

- (1) Tang, B.; Yu, F. B.; Li, P.; Tong, L.; Duan, X.; Xie, T.; Wang, X. *J. Am. Chem. Soc.* **2009**, *131*, 3016-3023.
- (2) Fan, L.; Liu, Q. L.; Lu, D. T.; Shi, H. P.; Yang, Y. F.; Li, Y. F.; Dong, C.; Shuang, S. M. *J. Mater. Chem. B*, **2013**, *1*, 4281–428.

